J. Theoret. Neurobiol. 2, 127–153 (1983)
Printed in Australia

DIFFUSION APPROXIMATIONS FOR NEURONAL ACTIVITY INCLUDING SYNAPTIC REVERSAL POTENTIALS

FLOYD B. HANSON*
Department of Mathematics, University of Illinois at Chicago, Chicago, Illinois 60680, U.S.A.
and
HENRY C. TUCKWELL
Department of Mathematics, Monash University, Clayton, Victoria 3168, Australia.

(Received November 3, 1982; in final form, January 10, 1983)

Abstract

Diffusion approximations to a discontinuous Markov process representing the subthreshold depolarization of a model neuron are considered. The model includes exponential decay, random excitation and inhibition, synaptic reversal potentials and fixed threshold for firing. The first two moments of the depolarization in the absence of threshold are obtained for the discontinuous model and the diffusions, and, for the latter, expressions are obtained for the stationary densities. From the stationary densities it is possible to ascertain whether the firing rate will be in the physiological range. The mean and coefficient of variation of the interspike interval are calculated for the diffusion models by numerical and asymptotic methods. A comparison of these results is made with those from previous computer simulations for the discontinuous processes.

1. Introduction

A diffusion process that has often been used to model the subthreshold depolarization of a nerve cell is the Ornstein-Uhlenbeck process (Gluss, 1967; Johannesma, 1968; Roy and Smith, 1969; Capocelli and Ricciardi, 1971; Ricciardi and Sacerdote, 1979; Tuckwell and Cope, 1980; Wan and Tuckwell, 1982). This process is derived from Stein's (1965, 1967) model in which a cell receives random excitatory and inhibitory postsynaptic potentials of fixed amplitudes (which may be random). Between synaptic inputs the depolarization decays exponentially to zero. When the depolarization reaches a fixed threshold an action potential is emitted, whereupon the process starts anew.

It is well established that the change in the depolarization of a nerve cell when it receives synaptic input depends on the difference between the prior voltage and the synaptic reversal potential characteristic of the activated synapses. (For examples see Eccles, 1964, 1969.) For excitatory synapses the reversal potential is often roughly midway between the sodium and potassium potentials, whereas the inhibitory

*Supported in part by NSF grant numbers MCS 79-01718 and MCS 81-01698.

reversal potential is governed mainly by the values of the potassium and/or chloride Nernst potentials, depending on the transmitter and postsynaptic membrane.

The Discontinuous Model

The model we consider first has excitatory and inhibitory synaptic inputs occurring at the times of jumps in independent Poisson processes, $P_e(f_e;t)$ and $P_i(f_i;t)$, where f_e and f_i are the corresponding intensities. If the depolarization is V(t) at time t, then, for subthreshold values,

$$dV = -V dt + \sum_j a_j(V_j - V)dP_j. \tag{1}$$

where $\sum_j$ means sum over excitatory and inhibitory terms. Here V_e and V_i are the excitatory and inhibitory reversal potentials and the constants a_e and a_i are the postsynaptic potential amplitude coefficients. The threshold for firing is assumed a constant θ and time is in units of the membrane time constant.

In the above model, V(t) is discontinuous at the jump times of P_e and P_i. If t_1 is the time of a jump in P_j, then the magnitude of the jump in V is

$$V(t_1^+) - V(t_1^-) = a_j(V_j - V(t_1^-)). \tag{2}$$

Thus the amplitude of the psp's diminishes as the potential approaches the reversal potentials. A more complete theory would include discretization to the spatial sumation of psp's as done in Poggio and Torre (1978) or include more general nonlinear effects due to ionic conductance changes as in the well known Hodgkin-Huxley theory.

For V(t) defined by Eq. (1), the first and second infinitesimal moments are

$$M_1(v) = \lim_{\Delta t \to 0} \frac{E[\Delta V(t) | V(t) = v]}{\Delta t} \tag{3}$$

$$= -v + \sum_j a_j f_j (V_j - v).$$

$$M_2(v) = \lim_{\Delta t \to 0} \frac{\mathrm{Var}[\Delta V(t) | V(t) = v]}{\Delta t} \tag{4}$$

$$= \sum_j a_j^2 f_j (V_j - v)^2.$$

To find the moments of the interspike interval for this model one has to solve differential-difference equations with variable coefficients. For such equations solutions are very difficult by either numerical or asymptotic methods. It is therefore useful to turn to diffusion approximations for V(t) for which moments of the first passage time can be found more easily.

2. Diffusion Approximation

One method of obtaining a diffusion approximation, V*(t), to the process V(t) defined by Eq. (1) is to let V*(t) have the same first two infinitesimal moments as V(t),

as given in Eqs. (3) and (4). Such an approximation, called the *usual* approximation by Walsh (1981) will be defined through the (Ito) stochastic differential

$$dV^* = M_1(V^*)dt + M_2^{1/2}(V^*)dW, \tag{5}$$

where $W = \{W(t), t \geq 0\}$, is a standard Wiener process. The transition probability density function of V*, which for $s \leq t$ we denote by $p(v,t|u,s)$, satisfies the forward Kolmogorov equation

$$p_t = -(M_1(v)p)_v + \tfrac{1}{2}(M_2(v)p)_{vv}, \tag{6}$$

where subscripts t and v denote partial derivatives. Note that V*(t) has continuous sample paths in contrast with those of the original process V(t).

Boundary Classification and Conditions

In the absence of a threshold, the depolarization V(t) in the original model is constrained to the finite interval (V_i, V_e) between the reversal potentials if there is excitation and inhibition, provided V(0) is between V_i and V_e. Similarly, V(t) is constrained to $(0, V_e)$ when there is excitation only and V(0) is between 0 and V_e. In contrast, the approximation V*(t) defined by (5) takes values on the whole real line, providing no barriers are imposed (see below).

Before we can impose boundary conditions for (6) and related moment equations we need to *classify* certain boundaries for V*. The classification is important because $M_1(v)$ and $M_2(v)$ can be either zero or infinite at various values of v in $(-\infty, \infty)$. In particular, the classification depends on the integrability of four functionals of M_1 and M_2 (see for example, Karlin and Taylor, 1981). The first of these is the Wronskian

$$W(v) = \exp\left[-2\int^v du M_1(u)/M_2(u)\right]. \tag{7}$$

The integral of W is related to the probability that a boundary point v can be reached from the interior of some open interval. The other three functionals are $1/M_2W$, $W\int dv/M_2W$ and $(1/M_2W)\int dvW$, which are related to the stationary distribution, the mean time to exit from an interval and the mean time to enter an interval from a neighbourhood of one of its boundaries, respectively.

We give the classification of the boundaries in Table 1.

Table 1
Classification of the boundaries for the diffusion approximation

Boundary Point	*Parameter Values*	*Classification*	*Boundary Condition Employed*
V_i	$f_j, a_j > 0$	regular	reflecting
V_e	$f_j, a_j > 0$	regular	reflecting
V_e	$f_i, a_i = 0$	entrance	asymptotically reflecting
0	any	regular	reflecting
$+\infty$	$f_j, a_j > 0$	natural	asymptotically reflecting
$-\infty$	$f_j, a_j > 0$	natural	asymptotically reflecting
$-\infty$	$f_i, a_i = 0$	entrance	asymptotically reflecting
θ	$0 < \theta < V_e$	regular	absorbing

Also listed are the conditions that we impose if a boundary is regular (nonsingular) or that must necessarily be imposed otherwise.

The term asymptotically reflecting means that the probability flux approaches zero in the limit as the boundary is approached. For the case of excitation and inhibition ($f_j, a_j > 0$), other boundary conditions could be imposed at V_i and V_e, but reflecting is chosen as the most appropriate to mimic the nonregular behaviour of the original process. Similarly, when there is excitation only, we impose a reflecting condition at $v = 0$ in place of the natural boundary condition of the original process. Finally, the threshold θ, which is between 0 and V_e, is a regular point which must be an absorbing boundary.

3. Mean, Variance and Stationary Distributions

Although they do not relate to the firing time problem *per se*, there are certain quantities related to the random processes described above which are calculable, usually in closed form. These are the mean, variance and stationary distribution of the processes in the absence of threshold. The mean and variance can relate directly to experiment and the stationary densities are expected to be a guide to the magnitude of the moments of the time to firing.

The jump process with excitation only

When there is excitation only so that $a_i f_i = 0$, the process V(t) cannot go below the resting level $V = 0$. Thus V(t) is restricted between 0 and V_e as long as $u = V(0)$ is similarly restricted. The forward Kolmogorov equation for this case is, with $p(v,t|u,0)$ abbreviated to $p(v,t|u)$,

$$p_t = -(-vp)_v + f_e\left[\frac{p((v-a_eV_e)/(1-a_e),t|u)}{(1-a_e)} - p(v,t|u)\right]. \tag{8}$$

This partial differential-difference equation is very difficult to solve and we have not found a solution, even in the stationary limit as t becomes infinite, making $p_t = 0$. We can nevertheless find the mean and variance,

$$m_1(t) = E[V(t)|V(0) = u] \tag{9}$$

$$\mathrm{Var}(t) = \mathrm{Var}[V(t)|V(0) = u]. \tag{10}$$

From the Kolmogorov equation, the mean satisfies

$$m_1'(t) = -r(m_1(t) - m_1(\infty)),\ m_1(0) = u, \tag{11}$$

where

$$m_1(\infty) = f_e a_e V_e / r, \tag{12}$$

$$r = 1 + f_e a_e. \tag{13}$$

The solution of (11) is

$$m_1(t) = (u - m_1(\infty))e^{-rt} + m_1(\infty). \tag{14}$$

The second moment can be shown to satisfy

$$m_2'(t) = -sm_2(t) + 2r(1-a_e)m_1(\infty)m_1(t) + r^2m_1^2(\infty)/f_e,\ m_2(0) = u^2, \tag{15}$$

where

$$s = 2 + f_e a_e(2 - a_e). \tag{16}$$

The solution of (15) is

$$\begin{aligned} m_2(t) = [u^2 &- 2(1-a_e)rm_1(\infty)((u - m_1(\infty))/(s-r) + m_1(\infty)/s) \\ &- r^2m_1^2(\infty)/(sf_e)]e^{-st} \\ &+ 2(1-a_e)rm_1(\infty)[(u - m_1(\infty))e^{-rt} + m_1(\infty)(s-r)/s]/(s-r) \\ &+ r^2m_1^2(\infty)/(sf_e). \end{aligned} \tag{17}$$

The variance of V(t), $\mathrm{Var}(t) = m_2(t) - m_1^2(t)$, can be found from (14) and (17). Its steady state limit is simply

$$\mathrm{Var}(\infty) = m_1^2(\infty)/(sf_e). \tag{18}$$

The diffusion approximation on $(-\infty, V_e)$ with excitation only

Here there is no inhibition and we do not impose a reflecting barrier condition at zero. The infinitesimal moments are $M_1(v) = -v + f_e a_e(V_e - v)$ and $M_2(v) = f_e a_e^2(V_e - v)^2$. The mean and variance of the diffusion turn out to be equal for those for the jump process considered above. Here we can find an explicit expression for the stationary density, which is the solution of the ordinary differential equation obtained by setting $p_t = 0$ in Eq. (6). Integrating this equation gives a stationary density

$$p_{st}(v) = \frac{R^{rR+1}}{\Gamma(rR+1)V_e}\left(\frac{V_e}{V_e - v}\right)^{rR+2}\exp[-RV_e/(V_e - v)], \tag{19}$$

for $v < V_e$ and where $\Gamma(\cdot)$ is the gamma function and

$$R = 2/(f_e a_e^2). \tag{20}$$

The diffusion approximation on $[0, V_e)$ with excitation only

The diffusion approximation with excitation only has the same phase space as the original jump process if we put a reflecting barrier at zero depolarization. The equation for m_1 does not lead to a closed form solution in this case, but we may find the stationary density as

$$p_{st}^*(v) = \frac{\Gamma(rR+1)}{\Gamma(rR+1;R)}p_{st}(v),\ 0 < v < V_e, \tag{21}$$

where $p_{st}(v)$ is given by (19), and $\Gamma(\cdot;y)$ is the incomplete gamma function based on the domain (y,∞). The steady state mean for this case is

$$m_1^*(\infty) = V_e[1 - R\Gamma(rR;R)/\Gamma(rR+1;R)]. \tag{22}$$

The steady state variance in this case is given by

$$\text{(23)}\qquad \mathrm{Var}^*(\infty)=\frac{(RV_e)^2}{\Gamma(rR+1;R)}\left[\Gamma(rR-1;R)-\frac{\Gamma^2(rR;R)}{\Gamma(rR+1;R)}\right].$$

As for $f_e a_e^2\to\infty$, $p^*_{st}(v)\to p_{st}(v)$, hence $m_1^*(\infty)\to m_1(\infty)$ and $\mathrm{Var}^*(\infty)\to\mathrm{Var}(\infty)$, so that in this limit the mean and variance, for the case with the barrier, approach the common values of the jump and the unrestricted diffusion with excitation only.

However, as $f_e a_e^2\to 0$, the restricted process leads to an over estimate of the moments compared to the unrestricted diffusion process as illustrated by the limit of the ratio of the two densities,

$$\text{(24)}\qquad p^*_{st}(v)/p_{st}(v)\sim 1+0.5\,\mathrm{erfc}(\sqrt{2f_e})> \text{ as } f_e a_e^2\to 0,$$

upon using asymptotic approximations of $\Gamma(x)$ and $\Gamma(x;y)$ analogous to Stirling's approximation; and where erfc$(\cdot)$ is the complementary error function. Hence, the relative difference between the two densities can be great, particularly in the case of small amplitude coefficients, a_e (e.g., as in miniature end plate potentials, see Fatt and Katz, 1952).

In conclusion, we can say that the unrestricted diffusion approximation better approximates the jump process, when the criterion for comparison is that approximation which best approximates the moments of the original process.

The jump process with both excitation and inhibition

In the presence of both excitation and inhibition, the jump process V(t) will remain in (V_i, V_e) provided the process starts here. The infinitesimal parameters M_1 and M_2 are again given by (3) and (4), and with these the Kolmogorov Eq. (5) yields the same equation of the mean $m_1(t)$, Eq. (11) with solution (14), except that now

$$\text{(25)}\qquad r=1+\sum_j f_j a_j$$

and the steady state limit is

$$\text{(26)}\qquad m_1(\infty)=\sum_j f_j a_j V_j/r.$$

However, the second moment can not quite be written in the previous form because it satisfies

$$\text{(27)}\qquad \begin{aligned} m_2'(t)&=-s[m_2(t)-m_2(\infty)]+2[rm_1(\infty)-D\cdot A]\cdot[m_1(t)-m_1(\infty)],\\ m_2(0)&=u^2,\end{aligned}$$

where now

$$\text{(28)}\qquad s=2r-D,\ D=\sum_j f_j a_j^2 \text{ and } A=\sum_j f_j a_j^2 V_j/D.$$

The solution of (27) is found to be

$$\text{(29)}\qquad \begin{aligned} m_2(t)=m_2(\infty)&+[u^2-m_2(\infty)+\\ &+\frac{2}{s-r}(rm_1(\infty)-DA)(u-m_1(\infty))(e^{(s-r)t}-1)]e^{-st},\end{aligned}$$

with steady state value

$$\text{(30)}\qquad m_2(\infty)=\frac{1}{s}[D\cdot(A^2+B^2)+2m_1(\infty)(rm_1(\infty)-D\cdot A)],$$

where

$$\text{(31)}\qquad B^2=\sum_j f_j a_j^2(V_j-A)^2/D.$$

The steady state variance can be simplified after some algebra to

$$\text{(32)}\qquad \mathrm{Var}(\infty)=\frac{1}{s}[D\cdot(B^2+A^2)+D\cdot m_1(\infty)(m_1(\infty)-2\cdot A)].$$

The diffusion approximation on $(-\infty,\infty)$ with both excitation and inhibition

In the presence of both excitation and inhibition the diffusion coefficient $\frac{1}{2}M_2(v)$ does not vanish at either reversal potential, V_e or V_i; and thus V_e and V_i do not form natural barriers for the diffusion process. The diffusion process of $(-\infty,\infty)$ has the same mean and variance as the jump process with both excitation and inhibition. However, the diffusion process has the following stationary density,

$$\text{(33)}\qquad p^*_{st}(v)=C\exp[R_2\,\mathrm{atan}(x)]/[1+x^2]^{R_1},$$

where atan$(\cdot)$ is the inverse tangent and

$$\text{(34)}\qquad x=(v-A)/B$$

is a normalized, natural variable which arises upon completing the square in $M_2(v)$. The other new parameters introduced in (33) are

$$\text{(35)}\qquad R_1=1+r/D,$$

$$\text{(36)}\qquad R_2=2r(m_1(\infty)-A)/(B\cdot D)=2[\sqrt{f_e f_i}\,(a_i-a_e)-A/B]/D,$$

and C, a normalization constant chosen so that

$$\int_{-\infty}^{\infty} dv\ p^*_{st}(v)=1,$$

which if needed can be written in terms of a beta function of a complex argument,

$$C=\frac{2^{2(R_1-1)}(2R_1-1)}{\pi B}\,\mathrm{Beta}(R_1-iR_2/2,\ R_1+iR_2/2).$$

Note that A and B can be considered as combined discrete-type mean and variance of the reversal potentials V_j with weights $f_j a_j^2$. The parameter R_1 is primarily the mean of $1/a_j$ and R_2 is related to the mean of V_j/a_j. In our study it turns out that both coefficients R_1 and R_2 will be relatively large and we will use this fact later for an asymptotic approximation of the mean interspike intervals.

The diffusion approximation on (V_i, V_e) *with both excitation and inhibition*

In this case we impose reflecting barriers at the reversal potentials V_i and V_e so that the diffusion process will be restricted to (V_i, V_e). The governing differential equations for the mean and the variance are not useful because they do not form a closed system in that we would need to know the probability densities at the reflecting barriers. The steady state density has the same form (33) as in the prior case,

$$p_{st}^*(v) = C^* \exp[R_2 \operatorname{atan}(x)]/[1+x^2]^{R_1}, \tag{37}$$

differing only in the normalization constant C^*, which is determined from the relation,

$$\int_{V_i}^{V_e} dv\, p_{st}^*(v) = 1,$$

at least in principle. Assuming that C^* is known we can formally compute the steady state value of the mean,

$$m_1^*(\infty) = A + \frac{B \cdot R_1}{2 \cdot R_3} - \frac{C^* \exp[R_2 \operatorname{atan}(\sqrt{R_4})]}{(1+R_4)^{R_3}} \left[1 - \frac{\pi R_2 R_4^{R_3}}{2}\right], \tag{38}$$

where $R_3 = (r-1)/D$ and $R_4 = f_i a_i^2/(f_e a_e^2)$. This mean appears to be quite different from the corresponding mean that arises in the unrestricted diffusion approximation and the jump process for both excitation and inhibition.

4. The Mean Interspike Interval for the Diffusion Approximation

If we ignore the refractory period, the mean interval between neuronal spikes will be the expected time to reach the threshold θ from a given initial depolarization u in the interval (V_i, θ) where $0 < \theta < V_e$. The time for the process $V^*(t)$ to reach θ is defined by

$$t_\theta(u) = \inf[t \mid V^*(t) \text{ not in } (V_i, \theta),\ V^*(0) = u] \tag{39}$$

and the n^{th} moment of the interspike interval (ISI) is denoted by

$$T_n(u) = E[t_\theta^n(u)],\ n = 0, 1, \ldots \tag{40}$$

$T_n(u)$ satisfies a backward equation (see Darling and Siegert (1953))

$$\tfrac{1}{2} M_2(u) T_n''(u) + M_1(u) T_n'(u) = -n T_{n-1}(u),\ u < \theta, \tag{41}$$

where M_1 and M_2 will be in general given by Eq. (3) and Eq. (4), respectively. Recall that the decay time constant is normalized to unity so that $T_1(u)$ is measured in units of the time constant, just as the frequencies f_j are measured in units of the reciprocal

time constant. The threshold θ in all cases will be an absorbing barrier, so that the threshold will be always attained with probability one, i.e., $T_0(u) = 1$. The boundary condition for instant absorption at θ is then $T_n(\theta) = 0$ for $n > 0$. The condition at the lower boundary, V_L, will depend on its location and on whether or not there is inhibition. The possible values that the lower boundary will assume in this paper are V_i, 0 and $-\infty$. In all cases, either reflecting or asymptotically reflecting conditions are used so that $T_n'(V_L^-) = 0$ for all right-handed limits $u \to V_L^-$. The asymptotically reflecting condition is guaranteed by the boundedness of $T_n(u)$. With this notation, we can write the solution to Eq. (41) after two quadratures in the single form:

$$T_1(u) = 2\int_u^\theta dz W(z) \int_{V_L}^z dy / M_2 W(y),\ V_L < u \le \theta \tag{42}$$

where $W(u)$ is the Wronskian defined in Eq. (7). Similarly, the second moment integrates to

$$T_2(u) = 4\int_u^\theta dz W(z) \int_{V_L}^z dy T_1(y) / M_1 W(y),\ V_L < u \le \theta. \tag{43}$$

The mean ISI for the diffusion approximation with both excitation and inhibition

The integrals representing the solutions to $T_1(u)$ in (42) and $T_2(u)$ in (43) cannot be found exactly. Numerical or asymptotic approximations are necessary to extract quantitative information from them. Both types of approximations have their advantages and disadvantages. In this section we summarize the numerical and asymptotic methods. Some more details of the asymptotic methods are given in an appendix.

The finite differencing of a single integral is quite straightforward, but multi-dimensional integrals can add other complications (Stroud, 1971). The integral in (43) for T_1 is a double integral. The integral in (43) for T_2 is nominally double, but is effectively a four dimensional integral. This is because the T_1 in integrand of (43) must be known to a higher degree of accuracy than we would desire for T_1 itself in order that T_2 be known to a comparable degree of accuracy as desirable for T_1 itself. When the domain is infinite as on $(-\infty, \theta)$, extra care must be taken to account for the singular behaviour. When the domain is finite as on (V_i, θ), multiple use of Gauss-Legendre quadrature (Stroud and Secrest, 1966) with its maximal polynomial precision is used to minimize the number of approximation points for desired accuracy. When the domain is infinite, it is convenient for the purpose of comparison to the finite domain results to only find the additional contribution from the tail on $(-\infty, V_i)$ that is needed to add to the finite domain result on (V_i, θ) In terms of the natural variable $x = (v - A)/B$, where A is given by (28) and B by (31), Eq. (42) takes the form,

$$T_1(A + Bx) = \frac{2}{D}(S_1 + S_{1T}), \tag{44}$$

with

$$(45)\qquad S_1=\int_x^{x_t}dzG_1(z)\int_{x_i}^{z}dyG_2(y),$$

$$(46)\qquad S_{1T}=\int_x^{x_t}dzG_1(z)\int_{-\infty}^{x_i}dyG_2(y),$$

$G_1(x)=C(1+x^2)/p^*_{st}(A+Bx)$, $G_2(x)=p^*_{st}(A+Bx)$, $x_t=(\theta-A)/B$ and $x_i=(V_i-A)/B$. All integrals in the finite domain part, S_1, and the tail part, S_{1T}, are approximated by a 16-node Gauss-Legendre quadrature, except for the second integral in (46). The second integral in (46) is singular and the form of the integral motivates the following transformation,

$$(47)\qquad y=\tan((\operatorname{atan}(x_i)+\pi/2)\exp(-y')-\pi/2,$$

which takes $(-\infty,x_i)$ in y into $(0,\infty)$ in y′ and introduces the standard Gauss-Laguerre weight factor, $\exp(-y')$ into the integrand. Upon making this transformation, an 8-node Gauss-Laguerre quadrature (Stroud and Secrest, 1966) is used to properly approximate the singular integral. The four dimensional integral for T_2 can be treated in a similar way except that the tail contribution has many more parts. The numerical results are discussed in Section 5.

The numerical results can be produced with sufficient accuracy except when an integrand becomes concentrated at isolated points or lines. When such concentration occurs, asymptotic methods may become just as suitable as, or even more suitable than, the nonadaptive numerical methods. We will study the asymptotic behaviour of the integrands in (42) and (43) using a two-dimensional extension of Laplace's method (Hanson and Tier, 1982). In this method we examine the integrand in exponential form,

$$(48)\qquad T_1(A+Bx)=\frac{2}{D}\int_x^{x_t}dz\,\exp[R_1h_1(z)]\int_{x_L}^{z}dy\,\exp[R_1h_2(y)],$$

where x_L is either x_i, $-A/B$ or $-\infty$ and where the exponents are given by

$$(49)\qquad R_1h_1(x)=(R_1-1)ln(1+x^2)-R_2\operatorname{atan}(x)$$

and

$$(50)\qquad R_1h_2(x)=R_2\operatorname{atan}(x)-R_1\,ln(1+x^2)=-R_1h_1(x)-ln(1+x^2).$$

Johannesma (1968) gives an unnormalized version of (48) with (49) and (50). For the typical data that we will use in Section 5, R_1 ranges from about 9 to 50 and R_2 ranges from about 9 to 30, provided that the IPSP's occur with sufficient frequency. While these values are not extremely large, they are fairly large for exponents. We will assume for the asymptotic methods that both parameters are asymptotically large, i.e., $R_1\gg1$ and $R_2\gg1$. Our technique is to examine the total exponent,

$$(51)\qquad h(y,z)=h_1(y)+h_2(z),$$

for critical points and maxima. The only interior critical point occurs at

$$(52)\qquad (y_c,z_c)=(R_2/2R_1,\ R_2/2(R_1-1)).$$

In the range of parameters considered, R_2 is approximately the same order as R_1, so that y_c and z_c range between 0.1 and 1.0 as long as f_i is between 0.2 and 2.0. The critical point (y_c,z_c) is a saddle or mini-max associated with the stochastic nature of the problem. Because a saddle cannot be the location of a global maximum or minimum, the direction of the gradient of h implies that the maximal contribution must be found at the boundary. The main contributing boundary points are those where the gradient of h is perpendicular to the boundary and its nearby projection on the boundary pointing toward the point in question. In the typical case, when y_c is sufficiently less than x_t, the principal maximum contribution occurs at the isolated boundary critical point $(y,z)=(y_c,x_t)$. A subsidiary set of critical points occurs along the line $y=z$ when $z\le z_c$ and we call this the critical manifold (CM). The critical manifold is associated with the deterministic component of T_1. The location of the critical points is given for a typical case in Figure 1. For asymptotic purposes the domain is split with three regions. The region PC with $x_{im}<z<x_t$ is the domain of influence of the principal contributing critical point, CM with $x_i<z<x_{cm}$ is the region of influence of the critical manifold and IM with $x_{cm}<z<x_{im}$ is an intermediate region containing the saddle (y_c,z_c). The cutoff points x_{im} and x_{cm} are determined by matching solutions by way of matching their errors.

The critical parameters y_c and z_c given in (52) have physical meanings. The stationary distribution written in terms of the x variable is

$$(52A)\qquad p^*_{st}(x)=C'\exp[R_1h_2(x)].$$

y_c is the maximum of p^*_{st} because it is the maximum of $h_2(x)$. Thus y_c is the mode or maximum point of the stationary distribution. On the other hand, z_c appears as the turning point of the backward differential equation (41); or more simply put, it appears as the attracting equilibrium point of a quasi-deterministic approximation,

$$(52B)\qquad \dot X(t)=D\cdot(R_1-1)(z_c-X(t)),$$

that omits the diffusion term in (5) (the actual deterministic model is $\dot V(t)=-V(t)$). The parameters are typically very close together for large R_1 because $z_c=y_c/(1-1/R_1)$.

The leading order distribution is obtained by expanding about the principal critical point, (y_c,x_t) to first order for h_1 and second order for h_2 in the exponent of the integrand of (48),

$$(53)\qquad T_1(A+Bx)\sim T_{1pco}(x)=C_{1pco}\cdot[1-\exp(-R_1g_{tx})],$$

where

$$(54)\qquad C_{1pco}=\frac{2\exp[R_1(h_1(x_t)+h_2(y_c))]}{D\,R_1^{3/2}\,h_1'(x_t)}\sqrt{\frac{2\pi}{-h_2''(y_c)}}$$

and

$$(55)\qquad g_{tx}=h_1'(x_t)\cdot(x_t-x).$$

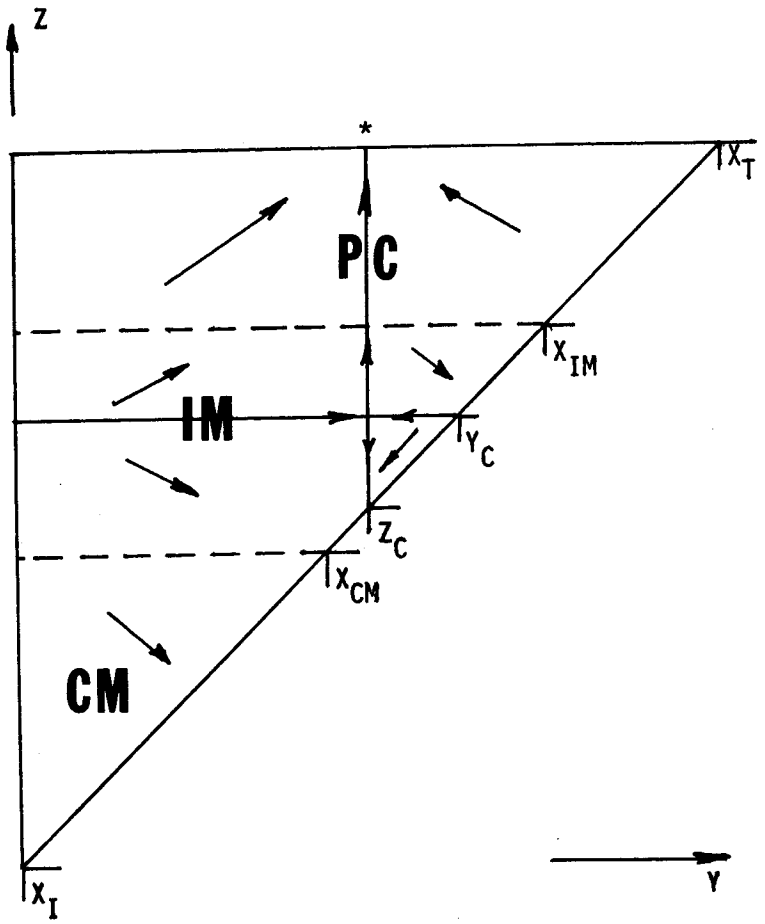

Fig. 1. Asymptotic regions for T_1 in the typical case. The arrows indicate the direction of the gradient of h(y,z). The asterisk (*) indicates the location of the principal contribution.

Equation (53) is valid as long as $y_c < x_{im} < x_t$. The approximation of the inner integral in (48) is independent of the limits of integration, so that (53) is valud for both domains, $(-\infty,\theta)$ and (x_i,θ). The limits of the outer integral of (48) have been retained in order to have dependence on x and to satisfy the boundary condition at the threshold. A similar approximation of

$$(56) \qquad T_2(A+Bx) = \frac{4}{D}\int_x^{x_t} dz \int_{x_L}^{z} dy \, \exp[R_1(h_1(z)+h_2(y))]T_1(A+By),$$

picks out the value of T_1 in the integrand at y_c, so that

$$(57) \qquad T_2(A+Bx) \sim T_{2pco}(x) \equiv 2 \cdot T_{1pco}(y_c) \cdot T_{1pco}(x).$$

The coefficient of variation has the corresponding approximation:

$$(58) \quad CV(A+Bx) = \sqrt{T_2/T_1^2 - 1} \sim \sqrt{2(1-\exp(-R_1 g_{tyc}))/(1-\exp(-R_1 g_{tx})) - 1}.$$

The approximations for T_1 in (53), T_2 in (57) and CV in (58) require extremely little computational effort. Both (53) and (57) can be exponentially large if R_1 is very large, but in typical neuronal cases R_1 is not very large so that the main problems with these formulae are that they may not be accurate enough or that PC is too small. Higher order corrections may be needed and we have placed some of the technical details of higher order approximations in an appendix. We compare these asymptotic results to the numerical results in Section 5.

The mean ISI for the diffusion approximation with excitation only

When there are only excitatory psp's, $f_i = 0$ and the forward Kolmogorov equation is singular at $v = V_e$ because $M_2(v)$ vanishes there. Hence the limit $f_i \to 0^+$ is singular. The numerical and asymptotic methods previously discussed carry over to this case anyway, provided we reinterpret the parameters.

$$(59) \qquad A = V_e,\ B = V_e - \theta,\ D = f_e \cdot a_e^2,\ R_1 = 1 + (1 + f_e a_e)/D \text{ and}$$
$$R_2 = -2V_e/(D \cdot B),$$

and exponents,

$$(60) \qquad R_1 h_1(x) = 2 \cdot (R_1 - 1) \cdot ln|x| + R_2/x,$$

and

$$(61) \qquad R_1 h_2(x) = -R_2/x - 2 \cdot R_1 ln|x|.$$

The asymptotic formulae (53), (57) and (58) now hold for excitation with and without inhibition, provided exponents (49) and (50) are used for the former and (60) and (61) are used for the latter. Note that the latter pair of formulae are not simple limits of the former pair. The parameter choice (59) for the excitation only case is crucial in generalizing our methods to both cases.

5. Results and Discussion

In this section numerical and asymptotic results are presented for the expected interspike interval as well as the second moments and coefficient of variation. "Physiologically reasonable" values of the neural parameters are taken from an example of Tuckwell (1979), who reported the results of numerical simulations for the Poisson model (1) of a point neuron with reversals. Hence the parameter values used here are $V_i = -9$mV, $\theta = 9$mV, $V_e = 90$mV, $a_e = 1/30$ and $a_i = 1/3$. The psp amplitudes are each 3mV starting from the rest potential $V(0) = 0$. Three excitation frequencies, $f_e = 1/\tau$, $2/\tau$ and $3/\tau$, are used where τ is the unnormalized time constant (5.8 ms. is used in Tuckwell, 1979); while the frequency of inhibition ranges from $0./\tau$

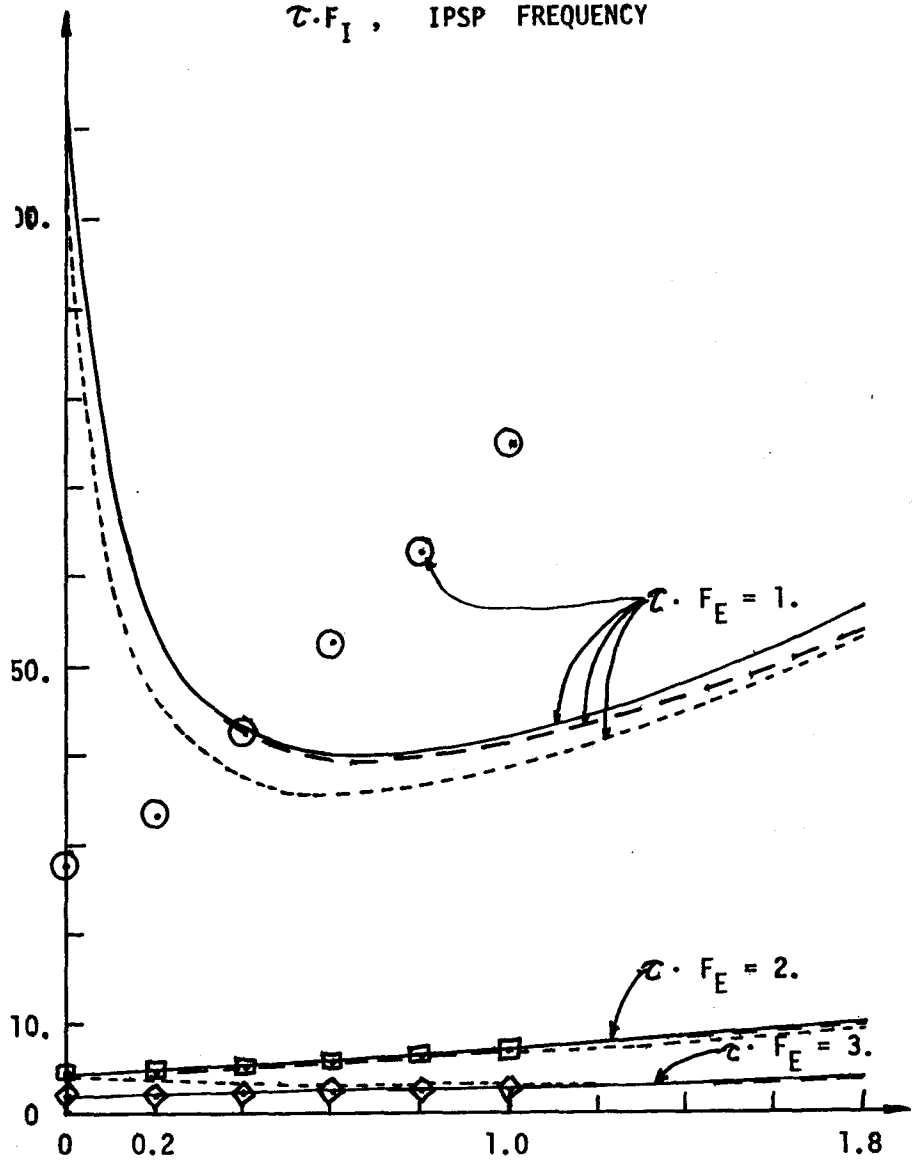

Fig. 2. A comparison of approximations for the expected interspike interval as a function of f_i with f_e as a parameter. The diffusion approximation on (V_i,θ) is indicated by a solid line for the numerical results, a long dashed line for the higher order asymptotic results and a short dashed line for the leading order asymptotic results. The circles, squares and diamonds are from the numerical simulations of the Poisson model (1) from Tuckwell (1979) for $\tau f_e = 1$, 2 and 3 respectively.

to $1.8/\tau$. Our results are exhibited with general time units of τ and frequency in units of $1./\tau$.

In Figure 2 the value of $T_1(0)/\tau$ is plotted versus τf_i. When $\tau f_e = 2$ or 3, the mean ISI has very close to linear dependence on f_i and there is good agreement among the numerical results, the higher order asymptotic results and the results of Tuckwell (1979). The leading order asymptotic approximation (53) compares quite well for $\tau \cdot f_e = 2$, but the result for $\tau \cdot f_e = 3$ deviates somewhat from the others as $f_i \to 0^+$ due to the fact that $x_{im} > x_t$ for $f_i \leq 1.0$; and as a result the domain of influence of the principal

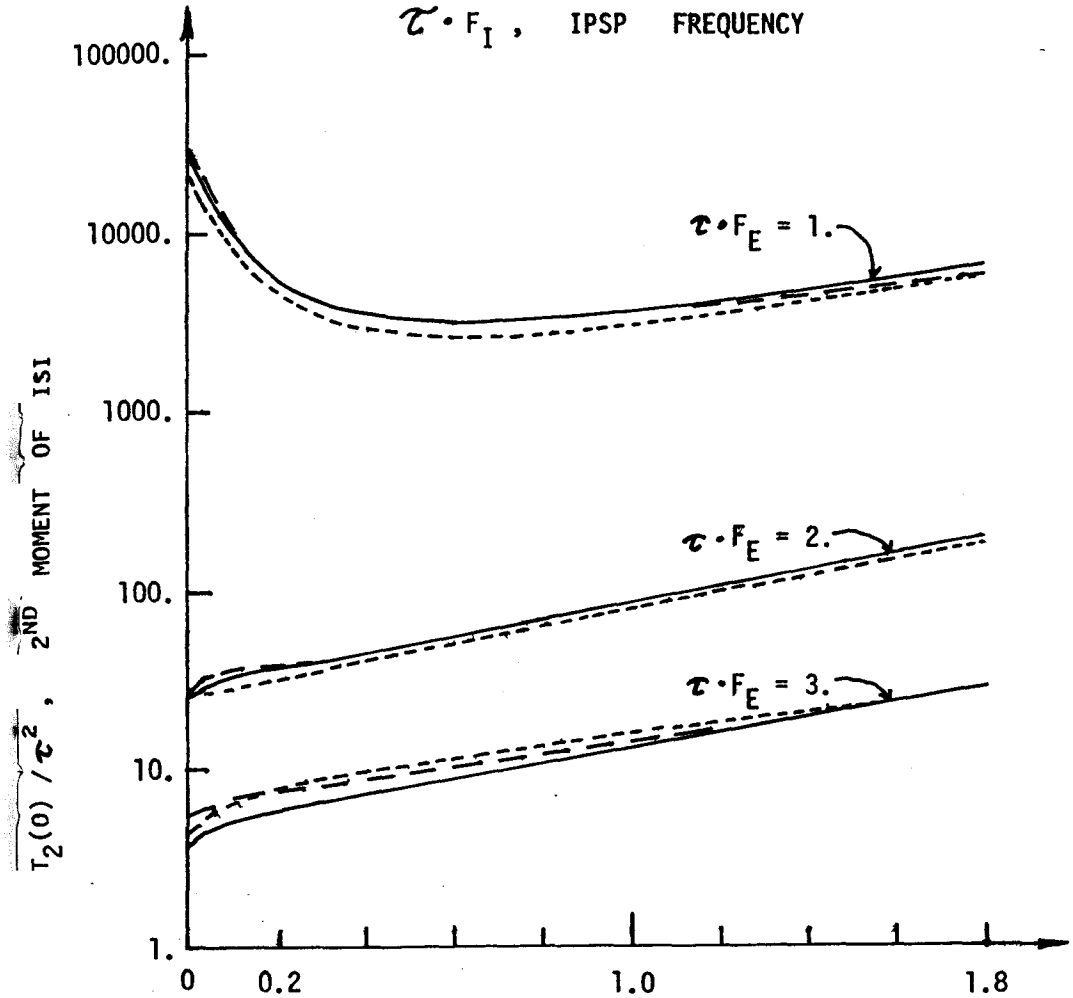

Fig. 3. A comparison of approximations for the second moment of the interspike interval as a function of f_i with f_e as a parameter. The legend is the same as that for Fig. 2.

critical point, (y_c,x_t), ceases to be important or becomes nonexistent. When $\tau\cdot f_e=1$ the numerical and asymptotic results for the diffusion approximation are in good agreement; they are first decreasing from $\tau\cdot f_i=0$ and then increasing from $\tau\cdot f_i\doteq 0.6$. In contrast the result of Tuckwell (1979) is strictly monotonically increasing. A plausible reason for this discrepancy might be the fact that the impact of the singular limit $f_i\to 0^+$ for the diffusion approximation is more pronounced for smaller excitation frequencies, while the original Poisson model does not have a similar singular limit as $f_i\to 0^+$. The percentage difference of the higher order asymptotic approximation from the numerical approximation ranges from $\pm 0.3\%$ to $+11\%$ with a mean of about 3%; while the leading order differs by 5 to 10% from the numerical if we exclude those values for which $x_{im}<x_t$. The numerical results are very good except near $f_i=0$ where R_1 is largest and the integrands are very likely to have concentrated maxima adverse to the numerical methods. The estimated numerical error in T_1 ranges from 2% at $\tau\cdot f_i=0.2$ to less than 0.01% at $\tau\cdot f_i=1.8$.

In Figure 3 similar results for the second moment are presented. When $\tau\cdot f_e=2$ or 3 the dependence of $\log(T_2(0)/\tau^2)$ on f_i is nearly linear except for a slight dip near the singular limit; while there is a unimodel minimum near $\tau\cdot f_i=0.6$ when $\tau f_e=1.0$. The agreement of the asymptotic results and the numerical results appears good in this semilog plot. However, the percentage difference of the higher order approximation for $T_2(0)/\tau^2$ from the numerical with inhibition is less than 8.2% for $\tau\cdot f_e=1.$, 6.4% for $\tau\cdot f_e=2.$ and 30% for $\tau\cdot f_e=2.$; while the leading order approximation (57) differs less than 24.% at $\tau f_e=1$, 6.% at $\tau f_e=2.$ and 39% at $\tau f_e=3.$ from the numerical. Although the accuracy of the asymptotic results is worse here when compared to the numerical computation, the asymptotic results for $T_2(0)$ at a single pair of frequencies (f_e,f_i) can be computed in a few seconds on an IBM 4341 while the numerical calculation takes about 3 minutes for $T_2(0)$.

In Figure 4, the coefficient of variation is plotted verses $\tau\cdot f_i$ for the values of $\tau\cdot f_e$. In general, the behaviour of the asymptotic results is poor compared to the numerical, much poorer than one would expect from the accuracy of T_1 and T_2 from which CV is calculated as in (58). In fact, the leading order approximation (58) does better on a greater percentage of frequencies than does the higher order approximation when the numerical results are used as a standard of comparison. The reason for this peculiar result is the way relative errors $\Delta T_1/T_1$ in T_1 and $\Delta T_2/T_2$ in T_2 propagate to the relative error $\Delta CV/CV$ in CV and this behaviour is approximately,

$$\Delta CV/CV\doteq 0.5(1+1/CV^2)(\Delta T_2/T_2-2\cdot\Delta T_1/T_1). \tag{62}$$

The relative errors of the leading order moments in (53) and (57) consistently approximately cancel each other. Those of the more complicated higher order approximation given in the Appendix can differ in sign, sometimes causing the tripling of the error from T_1 to CV and cancelling out at others. The comparison of the present numerical values of the CV to the simulation results of Tuckwell (1979) is only good for $\tau\cdot f_e=2$ and 3 when $\tau\cdot f_i$ is near 0. A similar problem with the propagation of error may be in operation here. The numerical results in the CV should

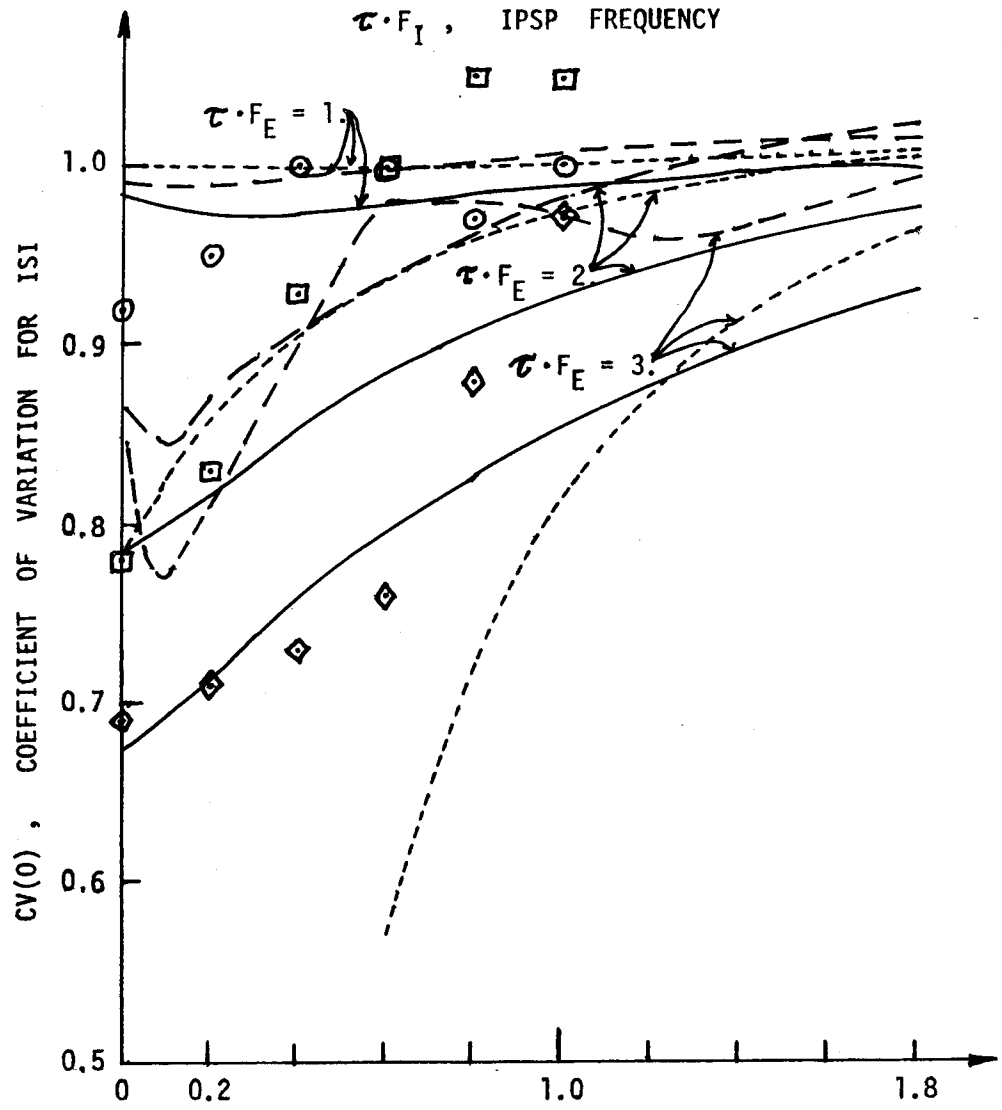

Fig. 4. A comparison of the approximations for the coefficient of variation for the interspike interval as a function of f_i with f_e as a parameter. The legend is the same as that for Fig. 2.

be good except near $f_i=0$ judging by the estimated accuracy of the numerical values of $T_1(0)$ and $T_2(0)$.

In Figure 5 the dependence of the expected first passage time for the threshold and its CV are illustrated as functions of the initial depolarization, $V(0)=u$, when

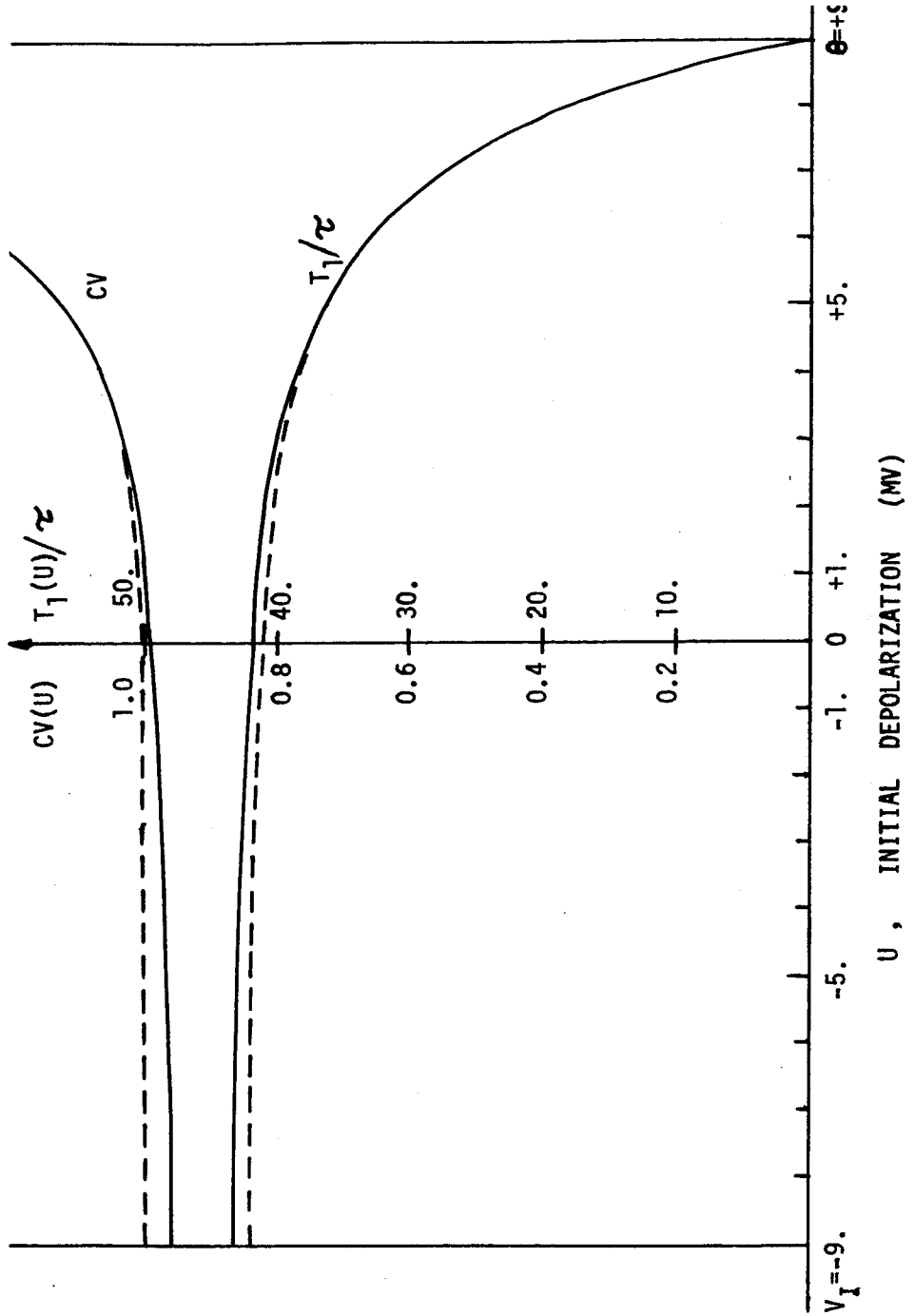

Fig. 5. The expected interspike interval and coefficient of variation versus the initial depolarization with $\tau f_e = 1$, $f_i = 1$ and the other parameters as stated in the text. The solid line indicates the numerical results for the diffusion approximation on (V_i,θ) and the dashed line the higher order asymptotic results.

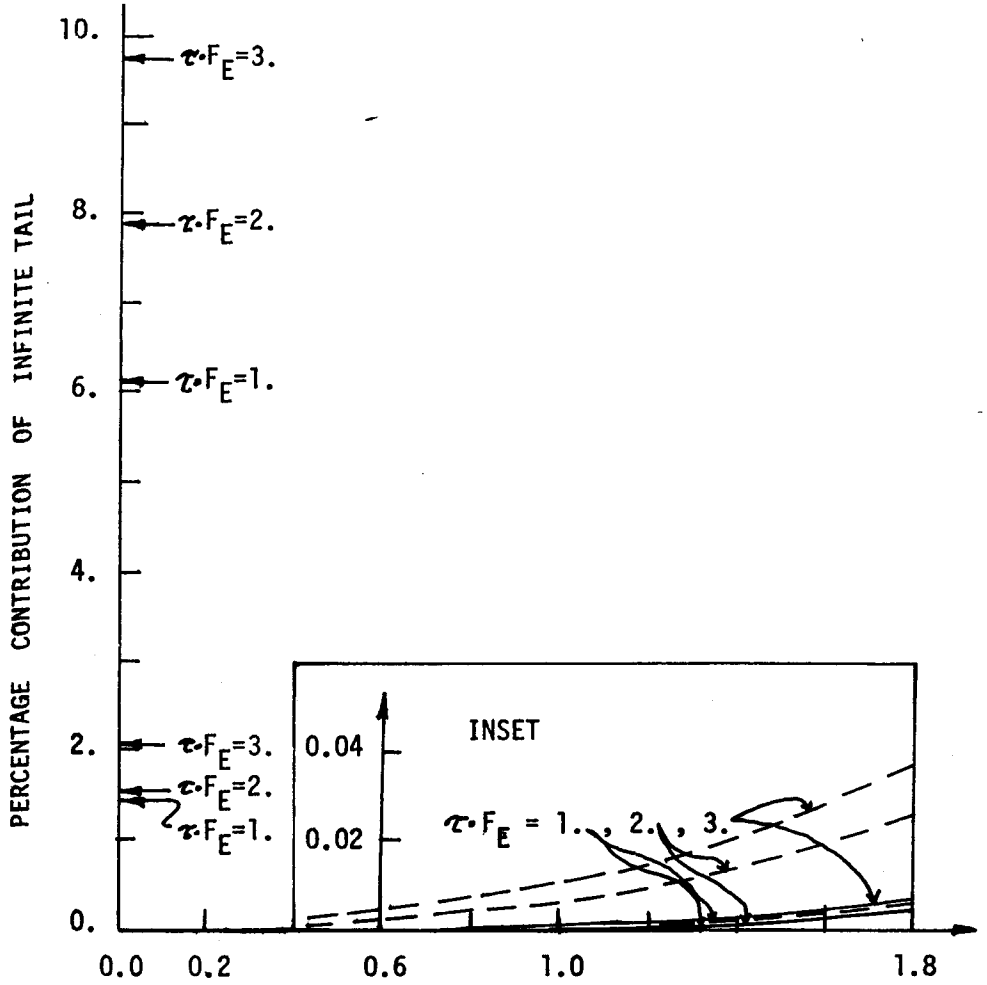

Fig. 6. The percentage contribution of the tail on $(-\infty,V_L)$ that must be added to the diffusion approximation of $T_1(0)/\tau$ on (V_L,θ) to obtain the result for $(-\infty,\theta)$. The solid line indicates the numerical approximation and the dashed line the higher order asymptotic approximation in the inset when $\tau f_i < 0$ and by the arrows when $\tau f_i = 0$.

$\tau \cdot f_i = 1 = \tau \cdot f_e$. The asymptotic and numerical results compare favorably. Although we are usually interested in the time of first passage from the rest state, $V(0) = 0$, the development of $T_1(u)$ with u can provide useful information about the time to threshold from any current value. For instance, suppose the depolarization has moved from $V = 0$ to $V = u$ at the current reset time $t = 0$, then $T_1(u)$ is the expected elapsed time to get from u to the spike threshold θ. For negative u, the logarithmic tail such as in T_{1cmz} of Equation (A20) is apparent; while the approach to the threshold is exponentially steep as in T_{1pco} of Equation (53) or T_{1pcp} of (A2). The CV varies slowly for negative u, but rises rapidly as the threshold is approached. This latter behaviour is caused by the first order zero of T_1 and T_2 when $u \to \theta^-$ resulting in $CV = 0(\theta - u)^{-0.5})$ as $u \to \theta^-$. This behaviour is a consequence of the neglect of the

absolute refractory period, p_r, which follows each firing of a neuron and prevents another firing until the refractory period is over. A simple device for including this phenomenon is to use $T_1 + p_r$ for the mean ISI instead of T_1 and $T_2 + 2p_rT_1 + p_r^2$ for the second moment instead of T_2 so that the corrected coefficient of variation,

$$(63) \qquad CV = [(T_2 - T_1^2)/(p_r + T_1)^2]^{0.5} = 0((\theta - u)^{+0.5}/p_r),$$

is bounded as well as vanishing as $u \to \theta^-$ instead of unbounded when there is no refractory period.

In Figure 6, the percentage contribution of the infinite tail, $(-\infty, V_i)$ to $T_1(0)$ is demonstrated. For excitation with inhibition, the contribution of this tail is negligible: less than 0.01% in the numerical approximation and less than 0.04% in the asymptotic approximation. The contribution of the tails to T_2 (not exhibited) are less than 0.08%. When there is no inhibition, then the numerical tail of T_1 contributes less than 2.1% while the asymptotic tail less than 10%. The values for T_2 are less than 4% in the numerical case and 13% in the asymptotic case. Hence the tail contribution can usually be neglected if there is sufficient inhibition, but the neglect of the tail contribution for T_1 and T_2 can still be considered with excitation only because the errors are in the range of those for the diffusion approximation itself. See Tuckwell and Cope's (1980) cautionary remarks about the accuracy of the diffusion approximation for excitation and inhibition without reversal potentials. The effect of inhibition on the tails is consistent with Stein's (1965) remark that the reversals are more important for inhibition.

However, for the purpose of making a simple qualitative appraisal of the effect of reversals on the full diffusion approximation, the leading order contribution (53) for the expected ISI with reversals (denoted by the dashed line) is compared in Figure 7 to the analogous leading order contribution of the expected ISI without reversals (denoted by X's connected by full lines). The analogous diffusion approximation without reversals is defined here by the first two moments,

$$(64) \qquad M_{1c} = M_1(0) \qquad \text{and} \qquad M_{2c} = M_2(0),$$

i.e. by taking the infinitesimal moments to be the constant (subscript c) values of (3) and (4) at the rest potential level. The leading order contribution analogous to (53) using the same asymptotic method is

$$(65) \qquad T_{1cpco}(0) = \frac{2\exp[H_{1c}(\theta) + H_{2c}(y_{cc})]}{D(B^2 + A^2)\, H_{1c}'(\theta)} \sqrt{\frac{2\pi}{-H_{2c}''(y_{cc})}} [1 - \exp[-H_{1c}'(\theta)\theta]]$$

where the simpler exponent functions are given by

$$(66) \qquad H_{1c}(v) = v(v - 2y_{cc})/[D(B^2 + A^2)] = -H_{2c}(v)$$

and with $y_{cc} = r\, m_1(\infty)$. An examination of Figure 7 shows that for $\tau \cdot f_e = 2$ or 3 there is very little absolute difference between the reversal and nonreversal cases, although the relative difference for $\tau \cdot f_e = 3$ can be big. In contrast, the qualitative difference when $\tau \cdot f_e = 1$ is very large, especially for the larger inhibitory frequency values. Therefore, we may qualify Stein's comment just mentioned to say that for the

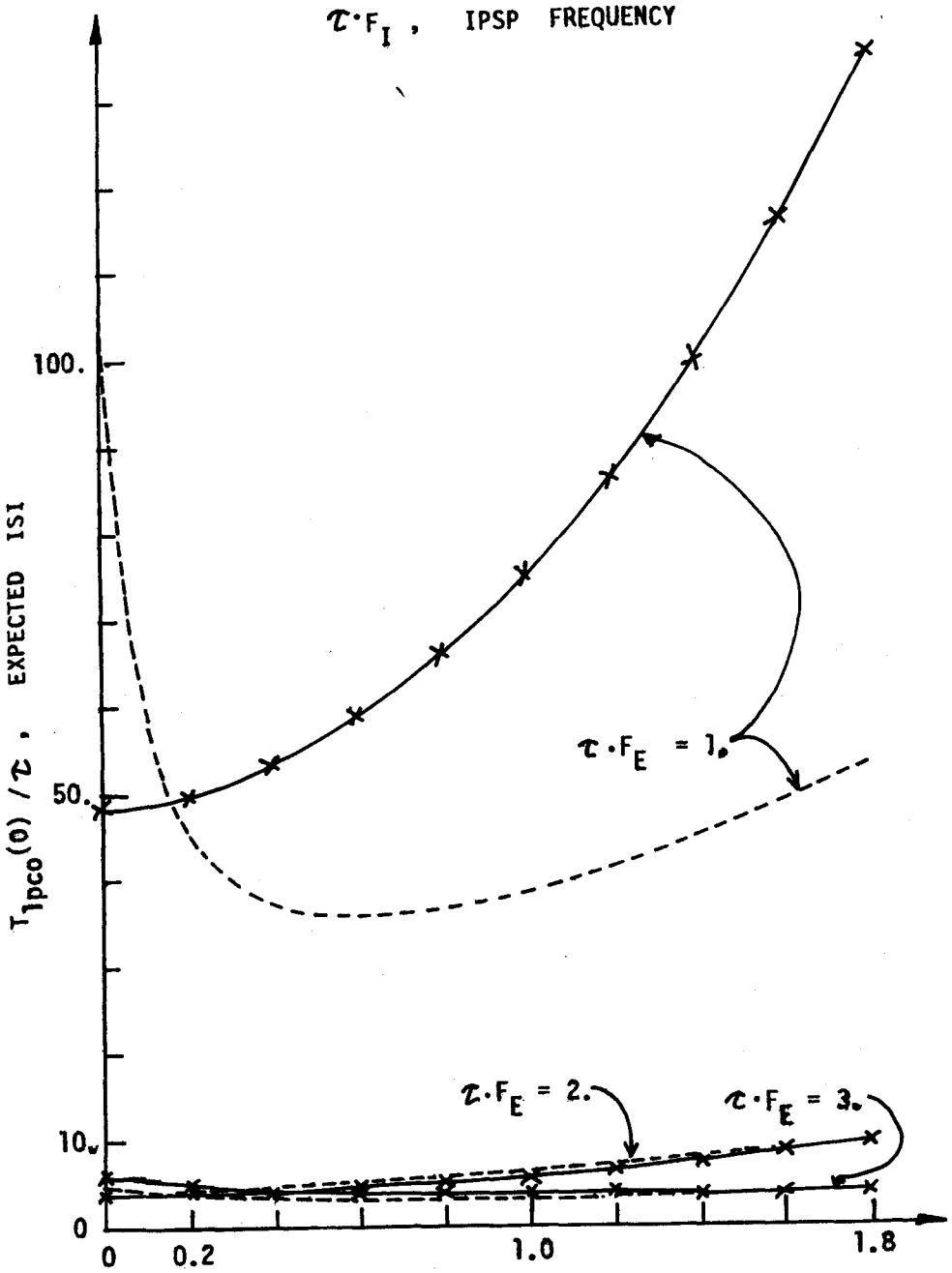

Fig. 7. A comparison of the diffusion approximation with and without reversals for the expected interspike interval as a function of f_i with f_e as a parameter. The reversal case, Eq. (53), is indicated by the dashed line and the nonreversal case, Eq. (65), by X's connected by full lines.

diffusion approximation the reversals are more important for inhibition in the lower range of excitatory frequencies.

The numerical and asymptotic results for the diffusion approximation of the mean interspike interval are quite good for sufficiently large excitation frequencies, $\tau \cdot f_e \geq 2$, in comparison to the results of the underlying Poisson model (1). However, caution must be used when considering the smaller values of $\tau \cdot f_e$ and also the coefficient of variation as an approximation to the original process. If the diffusion approximation is the process of interest, then the asymptotic approximations are quite suitable except for the CV and the computation takes much less time than the numerical methods. The simple leading order approximations in (53), (57) and (58) can be useful for qualitative behaviour provided care is taken to check that $x_t = (\theta - A)/B$ is sufficiently bigger than x_{im} given by (A23).

References

Capocelli, R. M. and Ricciardi, L. M. (1971). Diffusion approximation and first passage time for a model neuron. *Kybernetik* **8**, 214–223.

Darling, D. A. and Siegert, A. J. F. (1953). The first passage problem for a continuous Markov process. *Ann. Math. Stat.* **24**, 624–639.

Eccles, J. C. (1964). *The Physiology of Synapses.* Springer, New York.

Eccles, J. C. (1969). *The Inhibitory Pathways of the Central Nervous System.* Liverpool Univ. Press, Liverpool.

Fatt, P. and Katz, B. (1952). Spontaneous subthreshold activity at motor nerve endings. *J. Physiol.* **117**, 109–128.

Gluss, B. (1967). A model for neuron firing with exponential decay of potential resulting in diffusion equations for probability density. *Bull. Math. Biophys.* **29**, 223–243.

Hanson, F. B. and Tier, C. (1982). A stochastic model of tumor growth. *Math. Biosci.* **61**, 73–100.

Johannesma, P. I. M. (1968). Diffusion models for the stochastic activity of neurons. In: *Neural Networks* (E. R. Cainiello, Ed.), 116–144. Springer, New York.

Karlin, S. and Taylor, H. M. (1981). *A Second Course in Stochastic Processes.* Academic, New York.

Poggio, T. and Torre, B. (1978). A new approach to synaptic interactions. *Lecture Notes in Biomathematics* **21**, 89–115.

Ricciardi, L. M. and Sacerdote, L. (1979). The Ornstein–Uhlenbeck process as a model for neuronal activity. *Biol. Cybernetics* **35**, 1–9.

Roy, B. and Smith, D. R. (1969). Analysis of the exponential decay model of the neuron showing frequency threshold effects. *Bull. Math. Biophys.* **31**, 341–357.

Stein, R. B. (1965). A theoretical analysis of neuronal variability. *Biophys. J.* **5**, 173–194.

Stein, R. B. (1967). Some models of neuronal variability. *Biophys. J.* **7**, 38–68.

Stroud, A. H. (1971). *Approximate Calculation of Multiple Integrals.* Prentice-Hall, Englewood Cliffs, New Jersey.

Stroud, A. H. and Secrest, D. (1966). *Gaussian Quadrature Formulas.* Prentice-Hall, Englewood Cliffs, New Jersey.

Tuckwell, H. C. (1979). Synaptic transmission in a model for stochastic neural activity. *J. Theor. Biol.* **77**, 65–81.

Tuckwell, H. C. and Cope, D. K. (1980). The accuracy of neuronal interspike times calculated from a diffusion approximation. *J. Theor. Biol.* **83**, 377–387.

Walsh, J. B. (1981). Well-timed diffusion approximations. *Adv. Appl. Prob.* **13**, 352–368.

Wan, F. Y. M. and Tuckwell, H. C. (1982). Neuronal firing and input variability. *J. Theor. Neurobiol.* **1**, 197–218.

APPENDIX

In this appendix we will give a few of the technical details for the higher order asymptotic approximation in a form general enough to apply to the cases of excitation with and without inhibition. Concerning T_1 this higher order approximation consists of finding the leading order approximation in each region along with the next order correction for each term.

Approximation in the region PC

When $x_{im} < x < x_t$, the entire integration is in the principal contribution region PC. The main contribution T_{1pcp} in this region is from the critical point at (y_c, x_t), but there are two other terms due to the finiteness of the limits of integration at $y = z$ and $y = x_i$ or x_L in (48),

$$\text{(A1)} \qquad T_1(A+Bx) \sim T_{1pc}(x) = T_{1pcp}(x) + T_{1pcz}(x) + T_{1pci}(x),$$

where

$$\text{(A2)} \qquad T_{1pcp}(x) = \frac{2}{D}\int_x^{x_t} dz\, \exp[R_1 h_1(z)] \int_{-\infty}^{\infty} dy\, \exp[R_1 h_2(y)] \sim C_{tc} \cdot G_t(x)$$

with

$$\text{(A3)} \qquad G_t(x) = 1 - \exp(-R_1 g_{tx}) + C_t[1 - \exp(-R_1 g_{tx})(1 + R_1 g_{tx}(1 + .5 R_1 g_{tx}))] + \\ + \ldots,$$

$$\text{(A4)} \qquad C_{tc} = C_{1pco} \cdot \left[1 + \frac{h_2^{(4)}(y_c)}{8R_1[h_2''(y_c)]^2} - \frac{15[h_2^{(3)}(y_c)]^2}{72R_1[h_2''(y_c)]^3} + \ldots\right],$$

$$\text{(A5)} \qquad C_t = h_1''(x_t)/[R_1[h_1'(x_t)]^2];$$

the terms C_{1pco} and g_{tx} are defined in (54) and (55) respectively. Approximation (A2) is the direct higher order correction to our zero order result in (53) and is found by expanding the exponents, $h_1 + h_2$, out to several more terms in the spirit of a higher order Laplace approximation. The exponential term, $\exp(-R_1 g_{tx})$, is exponentially small except near the threshold boundary where it serves to guarantee that the boundary condition is satisfied there. Upon using integration by parts on the correction due to the $y = z$ boundary, we obtain

$$\text{(A6)} \qquad T_{1pcz}(x) = -\frac{2}{D}\int_x^{x_t} dz \int_z^{\infty} dy\, \exp[R_1(h_1(z) + h_2(y))]$$

$$\sim -\frac{1}{(R_1 - .5)D}\left[ln\left(\frac{x_t - y_c}{x - y_c}\right) - \frac{1}{(2R_1 + 1)h_2''(y_c)}\left(\frac{1}{(x - y_c)^2} - \frac{1}{(x_t - y_c)^2}\right) + \ldots\right]$$

The approximation (A6) is not of exponential order for $R_1 \gg 1$, but is singular as $x \to y_c^+$. This term may be interpreted as the contribution of the deterministic time from the threshold such as we would find from Equation (52B) with z_c approximated by y_c. On the other hand (A2) represents the time it takes to escape from the attracting point near $x = z_c \simeq y_c$. The third term on the right hand side of (A1) appears only when

there is a finite lower boundary $x_L = x_i$ or $-A/B$ and this term may also be approximated by a Laplace type expansion of the exponent of the integrand,

$$\text{(A7)} \qquad T_{1pci}(x) = -\frac{2}{D}\int_x^{x_t} dz \int_{-\infty}^{x_L} dy \exp[R_1(h_1(z)+h_2(y))] \sim -C_{ti}\cdot G_t(x)$$

where

$$\text{(A8)} \qquad C_{ti} = \frac{2\exp[R_1(h_1(x_t)+h_2(x_L))]}{DR_1^2 h_1'(x_t) h_2'(x_L)}\left[1+\frac{h_2''(x_L)}{R_1[h_2'(x_L)]^2}+\ldots\right]$$

and $G_t(x)$ is given in (A3). The approximation (A7) may be exponentially small or large, but exponentially less than the principal contribution in (A2).

Approximation in the region IM

When x is in the intermediate region $IM(x_{cm} \le x \le x_{im})$, the logarithmic correction from the boundary $y = z$ in (A6) becomes large and even unbounded because y_c is in the Region IM. Hence another approximation must be used in this region:

$$\text{(A9)} \qquad T_1(A+Bx) \sim T_{1im}(x) = T_{1pc}(x_{im}) + T_{1imz}(x) + T_{1imi}(x),$$

where $T_{1pc}(x_{im})$ is the contribution accumulated from T_{1pcp}, T_{1pcz} and T_{1pci} in (A2), (A6) and (A7) respectively at the point $x = x_{im}$ provided $x_t > x_{im}$. The main contribution from this region is obtained by stretching the variable z according to the change of variable

$$\text{(A9')} \qquad x'' = (z_c - x)/\delta_z \text{ with } \delta_z = \sqrt{2/R_1 h_1''(z_c)}$$

and the variable y according to

$$\text{(A10)} \qquad x' = (y_c - x)/\delta_y \text{ with } \delta_y = \sqrt{-2/R_1 h_2''(y_c)}$$

so that

$$\text{(A11)} \qquad T_{1imz}(x) = \frac{2}{D}\int_x^{x_{im}} dz \int_{-\infty}^{z} dy \exp[R_1(h_1(z)+h_2(y))] \sim C_{cc}\cdot[F_{imz}(x'') - F_{imz}(x_{im}'')],$$

where

$$\text{(A12)} \qquad C_{cc} = \frac{\delta_y \delta_z \exp[R_1(h_1(z_c)+h_2(y_c))]}{D},$$

$$\text{(A13)} \qquad F_{imz}(x) = K_1(x) - x[(\delta_z/\delta_y - 1)x - 2(z_c - y_c)/\delta_y] - R_1\delta_y^3 h_2^{(3)}(y_c)x(1+x^2/3)/6 - R_1\delta_z^3 h_1^{(3)}(z_c)[.5\sqrt{\pi} - (1-x^2)\exp(x^2)\operatorname{erfc}(x)) - x(1-x^2/3)].$$

The integral

$$\text{(A14)} \qquad K_1(x) = 2\int_0^x dz \exp(z^2)\int_z^\infty dy \exp(-y^2) = \sqrt{\pi}\, D_0(x) - x^2\cdot(1 + x^2/3\cdot(1+\ldots+2\cdot n x^2/(n+1)(2n+1)\cdot(1+\ldots))),$$

with the Dawson's integral

$$\text{(A15)} \qquad D_0(x) = \int_0^x dz \exp(z^2) = x\cdot(1 + x^2(1/3. + \ldots + x^2/n\cdot(1/(2n+1.) + \ldots))),$$

given here in Newton fast polynomial multiplication form, was also used by Wan and Tuckwell (1982) for the Ornstein and Uhlenbeck approximation to a neural model. Only for the case of finite lower boundary at $x_L = x_i$ or $-A/B$ is there also the additional term analogous to T_{1pci} in (A7),

$$\text{(A16)} \qquad T_{1imi}(x) = -\frac{2}{D}\int_x^{x_{im}} dz \int_{-\infty}^{x_L} dy \exp[R_1(h_1(z)+h_2(y))] \sim -C_{ci}\cdot[F_{imi}(x'') - F_{imi}(x_{im}'')],$$

$$\text{(A16)} \qquad C_{ci} = \frac{2\exp[R_1(h_1(z_c)+h_2(x_L)]\delta_z}{DR_1 h_2'(x_L)}\left(1+\frac{h_2''(x_L)}{R_1[h_2'(x_L)]^2}\right)$$

and

$$\text{(A18)} \qquad F_{imi}(x) = D_0(x) + \delta_z^3 R_1 h_1^{(3)}(z_c)(1-x^2)\exp(x^2)/12.$$

When x_t is in IM or x_t is sufficiently close to x_{im} then $T_{1imz}(x)$ becomes the global principal approximation with $x_{im} = x_t$ and this case does occur in some instances.

Approximation in the Region CM

When x is in the region $(x_L < x < x_{cm})$, the solution can be decomposed into

$$\text{(A19)} \qquad T_1(A+Bx) \sim T_{1cm}(x) = T_{1im}(x_{cm}) + T_{1cmz}(x) + T_{1cmi}(x)$$

with the first term on the right being the cumulative contribution from the approximations T_{1pcp}, T_{1pcz}, T_{1pci}, T_{1imz} and T_{1imi}. The main contribution in CM comes from the line $y = z$ like T_{1pcz} in (A6) and is approximated by integration by parts on the inner integral yielding,

$$\text{(A20)} \qquad T_{1cmz}(x) = \frac{2}{D}\int_x^{x_{cm}} dz \int_{-\infty}^{z} dy \exp[R_1(h_1(z)+h_2(y))] \sim \frac{+1}{(R_1 - .5)D}\left[ln\left(\frac{y_c - x}{y_c - x_{cm}}\right) - \frac{1}{(2R_1+1)h_2''(y_c)}\left(\frac{1}{(y_c - x_{cm})^2} - \frac{1}{(y_c - x)^2}\right) + \ldots\right],$$

which is also not exponentially large for $R_1 \gg 1$ and $x < x_{cm} < y_c$. For the finite domain, $x_L = x_i$ or $-A/B$ the tail correction is again approximated by a Laplace type expansion.

$$\text{(A21)} \qquad T_{1cmi}(x) = -\frac{2}{D}\int_x^{x_{cm}} dy \int_{-\infty}^{x_L} dy \exp[R_1(h_1(z)+h_2(y))] \sim -\frac{2\exp[R_1(h_1(x)+h_2(x_L))]}{DR_1^2 h_1'(x) h_2'(x_L)}\left[1+\frac{h_2''(x_L)}{R_1[h_2'(x_L)]^2}+\ldots\right]\cdot\left[1-\exp(-R_1 g_{mx}) + \frac{h_1''(x)}{R_1[h_1'(x)]^2}[1-\exp(-R_1 g_{mx})(1+R_1 g_{mx}(1+.5R_1 g_{mx}))]\right]$$

where

(A22) $g_{mx} = -h_1'(x)\cdot(x_{cm} - x).$

When x_t is in CM then $T_{1cmz}(x)$, (A20) becomes the global principal contribution with $x_{cm} = x_t$.

The form of the asymptotic solution given above for the first passage to threshold in the case of excitatory with and without inhibitory reversal potentials is qualitatively very similar to the form in Wan and Tuckwell (1982). However, their problem concerned the Ornstein–Uhlenbeck diffusion approximation for constant size excitatory psp's with inhibition (no reversal potentials). Their method was also different. Their method was also different. They used local type asymptotic methods on the differential equations, while our method is a global type because we worked with the integrated formal solutions.

Determination of the parameters x_{im} *and* x_{cm}.

The formulae for T_{1pcp}, T_{1pcz}, T_{1pci}, T_{1imz}, T_{1imi}, T_{1cmz} and T_{1cmi} should be suitable for approximating most cases asymptotically. However, the boundaries, x_{im} and x_{cm} of IM still need to be specified. These are determined by matching the approximations at x_{im} and x_{cm} by matching the worst errors between neighbouring regions. In particular, x_{im} is determined so that the worst error in region PC is the same order of magnitude as the worst error in IM. The worst error in PC is estimated by the first term neglected in the expansion of T_{1pcz} in (A6) because this expansion diverges in IM. The worst error in IM is estimated by the first term neglected in the expansion of T_{1imz} and these are the exponentially growing terms. Matching these errors gives

(A23) $x_{im} \sim y_c - \delta_z[-ln(\delta_z(-ln(\delta_z))^{1.5})]^{0.5}.$

Similarly, matching the worst errors from T_{1imz} with those of T_{1cmz} yields,

(A24) $x_{cm} \sim y_c - (x_{im} - y_c).$

Higher order approximations for T_2.

The asymptotic approximation of T_2 is similar to that of T_1 except that T_1 appears in the integrand of T_2 and that T_1 is piecewise approximated in different asymptotic regions. We will just give our formulae for T_2 in the region PC as an example.

When x is in (x_{im}, x_t),

(A25) $T_2(A+Bx) \sim T_{2pc}(x) = T_{2pcp}(x) + T_{2pcz}(x) + T_{2pci}(x),$

where

(A26) $T_{2pcp}(x) \sim 2\cdot T_{1im}(y_c)\cdot T_{1pcp}(x),$

(A27) $$T_{2pcz}(x) \sim 2\cdot C_{tc}\cdot T_{1pcz}(x) + \frac{1}{D(R_1+.5)h_1'(x_t)}\left[\frac{1}{x_t - y_c} - \frac{\exp(-R_1 g_{tx})}{x - y_c}\right] + \left[\frac{1}{D(R_1+.5)}\, ln\left(\left(\frac{x_t - y_c}{x - y_c}\right)\right)\right]^2 + \ldots,$$

and the optional tail correction is

(A28) $$T_{2pci}(x) = 2\cdot(T_{1pci}(y_c) + T_{1imi}(y_c))\cdot T_{1pcp}(x) - 2\cdot C_{ci}\left[(1+C_t)T_{1pcz}(x) + \frac{1}{(R_1+.5)Dh_1'(x_t)}\left(\frac{1}{x_t - y_c} - \frac{\exp(-R_1 g_{tx})}{x - y_c}\right)\right].$$

We have just given the major terms for each in order to keep the simplicity of the asymptotic approximation.